Transient oil-refrigerant mixture flow change after compressor shutdown at suction and discharge

Xin WANG[1], Nenad MILJKOVIC[1], Stefan ELBEL[2]*

[1]Air Conditioning and Refrigeration Center, Department of Mechanical Science and Engineering, University of Illinois at Urbana-Champaign, 1206 West Green Street, Urbana, IL 61801, USA

[2]Technische Universität Berlin, Institut für Energietechnik, FG Wärmeübertragung und -wandlung, Marchstr. 18, 10587 Berlin, Germany
* Corresponding Author: Stefan Elbel (email: elbel@tu-berlin.de)

ABSTRACT

The compressor oil is retained at different locations of the vapor compression system during operation. After shutdown, the retained oil absorbs the vapor refrigerant and mixes with the liquid refrigerant with temperature and pressure changes. In this paper, the liquid mixture behaviors after shutdown at the compressor suction and discharge are observed by flow visualization. The liquid mixture property variations are estimated with existing models according to the temperature and pressure variations. The refrigerant concentration in the liquid phase increases rapidly at suction after shutdown. The viscosity of the liquid decreases quickly with temperature and refrigerant mass fraction change. Flow visualization shows that the mixture film breaks from the top of the tube wall and flows down. Transient vapor condensation and re-evaporation occur with a sudden pressure increase. The oil-refrigerant mixture liquid level increases and decreases within seconds. At the discharge, the refrigerant solubility fluctuates within a small range. Viscosity increases because of temperature decrease then decreases because of refrigerant mass fraction increase. After shutdown, the oil flow in contact with the inner wall of the discharge stops immediately while oil droplets in the vapor core flow slow down gradually. Flow behaviors and property variations are compared after three different operation conditions. The results show that larger flow property changes and more severe vapor condensation happen at the suction with the higher outdoor temperature. The vapor refrigerant, liquid refrigerant, and oil relationship is investigated and estimated after shutdown to better understand oil retention.

1. INTRODUCTION

Oil is an essential component in the automotive air conditioning system. However, if oil migrates out of the compressor and is retained at other locations of the system, the system performance would be adversely affected in refrigerant distribution and COP penalty (McMullan *et al.*, 1992). To keep high-quality lubricant inside the compressor and reduce oil retention, many researchers have been working on oil flow behavior investigation.

Sethi and Hrnjak (2015) concluded that oil retention at the suction line can be influenced by many factors, such as gas superficial velocity, oil circulation rate (OCR), and different orientations of the tube. Haider *et al.* (2023a，2023b) showed that oil retention increases because of the refrigerant mass flux decrease and OCR increase. It was observed that the OCR of the system is influenced by the compressor speed and gas velocity (Haider，2023).

Stevanovic and Hrnjak (2017) presented that oil retention is closely related to the thermophysical and transport properties of the liquid mixture. Higher kinematic viscosity will lead to higher oil retention amount due to magnitude increase of viscous resistance. Cremaschi *et al*. (2005) pointed out that the oil retention is proportional to the liquid and vapor viscosity ratio. Besides, initial volume, driving force, and gravity force are aspects that can affect oil retention.

To quantify and predict oil retention at the suction line, numerical and experimental methods have been studied and applied. Radermacher *et al*. (2006) developed a numerical model to predict oil retention based on Navier-Stokes equation and interfacial shear stress friction factor. A wide range of refrigerants and oil is covered by this method. Sethi and Hrnjak (2015) used transparent tube to observe different flow regimes and correlated with oil retention measured by sampling method.

The oil retention at discharge has been quantified by Xu and Hrnjak (2017) with sampling and optical methods. At discharge, oil consists of oil film attached to the inner wall of the tube and oil droplets traveling in the vapor core of

the tube. The oil retention is mostly contributed to oil film at relatively low velocity. Liquid film thickness and film velocity are measured by a non-invasive critical angle method. It showed that with higher mass flux, oil film thickness gets smaller, and the oil retention from oil film is less.

According to the literature review above, oil retention is closely related to system working conditions and mixture properties. However, previous studies mostly focused on steady-state oil working conditions and flow characteristics. Flow behavior and mixture property change rapidly after shutdown, which has large effects on oil distribution. Peuker (2010) quantified refrigerant and oil mass distribution with experimental sampling method. The refrigerant quickly migrates from the high-pressure side to the low-pressure side after shutdown. Wang *et al*. (2023) presented that the refrigerant migration causes large working condition variations and differences between flow behavior at the suction and discharge.

Hence, this paper investigates working conditions and mixture property variations at the suction and discharge with validation of flow visualization. As observed, the oil stays as droplets at the inner wall of the tube after shutdown at the discharge. In contrast, oil film breaks from the top and flows down with refrigerant condensation at the suction after shutdown. The refrigerant solubility and mixture kinematic viscosity are estimated to explain the flow behaviors. Moreover, suction and discharge flow characteristics are studied and compared under 3 different working conditions to further understand oil retention under different conditions. The study of property variations and flow characteristics helps further understand oil retention reduction and oil return during startup.

2. EXPERIMENT DESCRIPTION

The experimental setup is composed of a compressor, condenser, EEV and evaporator. The schematic of the experimental facility is shown in Figure 1. An electrical scroll compressor for automotive applications is used in this study. The speed of the compressor can vary between 1100 min^{-1} and 2650 min^{-1}. R134a and PAG ISO 46 are used as refrigerant and lubricant for the experiment. An oil concentration sensor based on the speed of sound installed at the liquid line reports the real-time OCR data. OCR sampling method is also employed at the liquid line for validation.

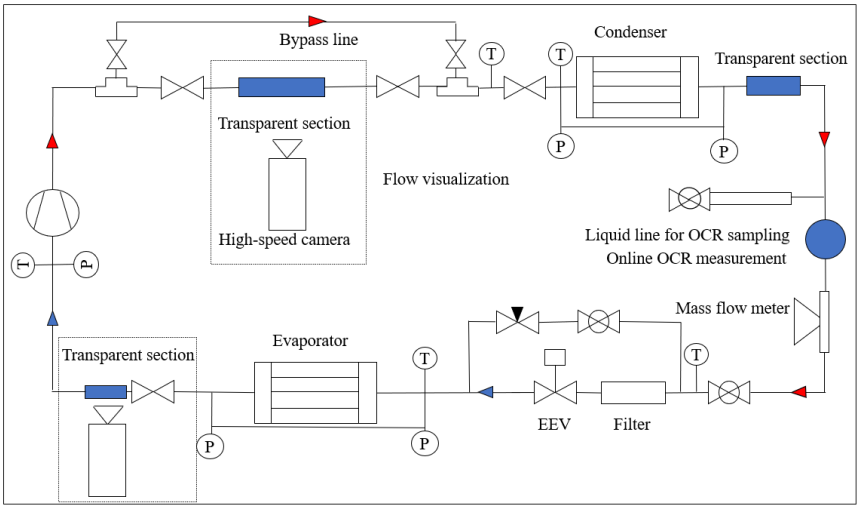

Figure 1. Schematic of experimental setup

Two environmental chambers are used to maintain the required conditions at the condenser and evaporator. The indoor and outdoor air-side temperatures are maintained at 24°C/39 °C during operation for normal tests (Condition B explained in the following section). The superheat at the evaporator outlet and subcooling at the condenser outlet are kept at 15 °C and 1.5 °C respectively. The mass flow rate of the system is measured by a Coriolis-effect mass flow meter. OCR varies with compressor speed from 1% to 2%. The gauge pressure transducers and T-type thermocouples are installed at the compressor inlet and outlet to measure the pressure and temperature change after shutdown. The uncertainties of measurement for the sampling method and visualization method are shown in Table 1.

Table 1. Measurement uncertainty

Measurement	Uncertainty
Temperature (°C)	±0.2
Pressure (kPa)	±3.5
Mass flow rate (g/s)	±0.2%
Tube geometry (mm)	±0.01
Weight by electronic balance (g)	0.01
OCR meter (%)	0.1%

Figure 2 shows the experimental setup layout. At the compressor suction and discharge, the flow visualization setups are established. Transparent perfluoroalkoxy (PFA) tubes are used to observe the flow behaviors at the discharge and the suction of the compressor. The inner diameters of the suction and discharge tubes are 6 mm (1/4 inch), the outlet diameters are 9 mm (3/8 inch), wall thicknesses are 1.5 mm (1/16 inch). The light sources from the LED panel behind the tube. A high-speed camera with lens is used to capture the transient flow. The location of flow visualization is 0.8 m downstream of the compressor. Facilities of visualization at the suction of the compressor are composed of LED light, PFA tube and high-speed camera as well. The tube is 0.5 m upstream of the compressor.

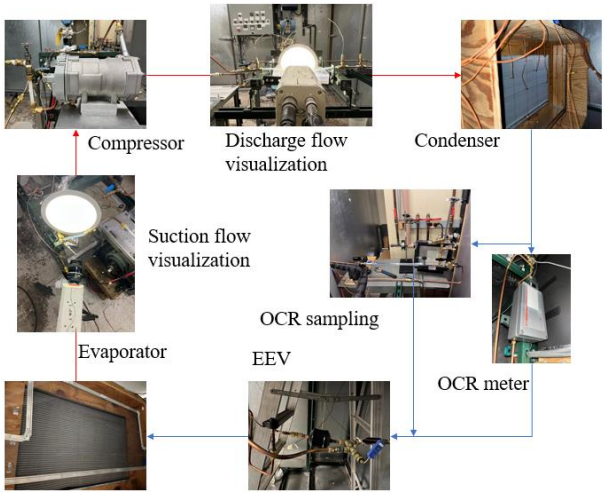

Figure 2. Main components of experiment facility

3. RESULTS

3.1 Suction and Discharge Lines of Compressor

Working condition and mixture property variations at the compressor suction and discharge are estimated and compared in this section. The flow visualization shows different oil-refrigerant mixture behavior after shutdown.

3.1.1 Working Conditions: The working conditions at the compressor suction and discharge are shown in Figure 3. After shutdown, the EEV and valves between the high- and low-pressure side are kept open during operation, which allows the refrigerant to migrate from the high-pressure side to the low-pressure side. As shown in Figure 3, the discharge pressure rapidly drops from 989 kPa to 740 kPa, and the suction pressure increases from 403 kPa to 740

kPa within 2 min after shutdown. After pressure equilibrium, the system pressure decreases with temperature change and heat transfer.

The discharge temperature gradually decreases from 63 °C to 30 °C within 38 min. The suction temperature quickly increases from 23 °C to 29 °C within 3 min, then gradually decreases to 26 °C.

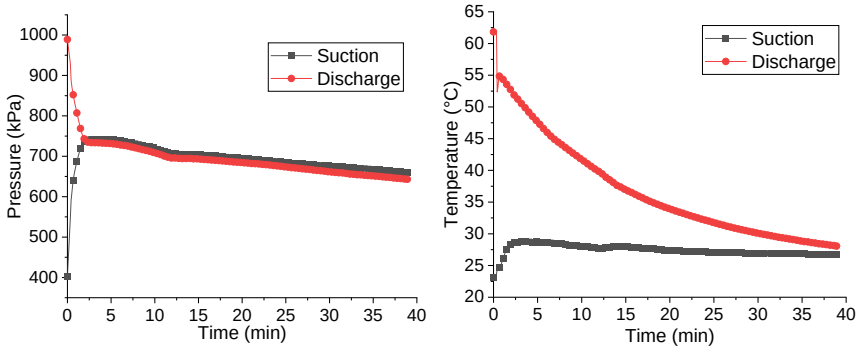

Figure 3. Pressure and temperature variation at compressor suction and discharge

Based on the pressure and temperature variations, the refrigerant superheat is calculated as shown in Figure 4. The superheat at the discharge slightly fluctuates within 1 min after shutdown, then decreases from 24 °C to 4 °C. The refrigerant stays as vapor refrigerant throughout the whole process. However, the superheat at suction suddenly drops from 14 °C to 0 °C within 1 min and remains at around 0 °C for 10 min. Therefore, the refrigerant starts to condense quickly after shutdown. The condensation and saturation of the refrigerant last 10 min. According to flow visualization, the liquid refrigerant potentially condenses on the inner wall of the tube and flows down. Due to the rapid change of the pressure and temperature, the saturation of the liquid refrigerant happens simultaneously.

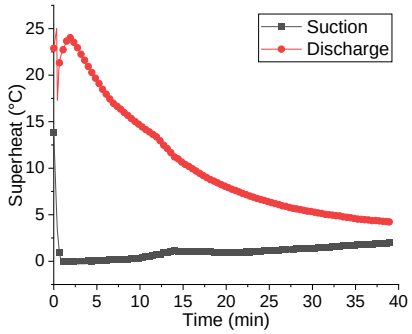

Figure 4. Superheat at compressor suction and discharge

The working condition variations at the suction and the discharge indicate the difference in the flow behavior at the low- and high-pressure side. At the suction, the pressure rapidly increases within the first 2 min, and thermal equilibrium takes a longer time to reach. The superheat acutely decreases to 0 °C since the pressure and thermal equilibrium are not synchronized. Considering the oil film thermal resistance between the tube wall and vapor, the temperature of the inner wall of the tube might be lower than the temperature of the tube core. The vapor refrigerant tends to condense at the tube wall.

At the discharge, the temperature and pressure decrease gradually in the longer term. Although the superheat decreases rapidly after the shutdown, the refrigerant is always in the vapor phase.

3.1.2 Mixture Properties: The refrigerant solubility in oil and the mixture kinematic viscosity are calculated based on temperature and pressure variations as shown in Figure 5. A steady-state empirical model of R134a-PAG oil solubility presented by Grebner (1992) is applied to predict refrigerant mass fraction as Equation (1) to (4). However, the model is limited to superheated refrigerant and liquid oil. The superheat plot in Figure 4 shows that the refrigerant at the suction condenses from 1 min after shutdown and lasts for 1.5 min, which results in the gap of the refrigerant mass fraction curve.

$$T^* = (1 - w_r)[A(w_r) + B(w_r)p] \qquad (1)$$

where

$$T^* = \frac{T - T_{sat}(p)}{T_{sat}(p)} \quad (2)$$

$$A(w_r) = a_0 + \frac{a_1}{{w_r}^{1/2}} \quad (3)$$

$$B(w_r) = b_0 + \frac{b_1}{{\omega_r}^{1/2}} + \frac{b_2}{\omega_r} + \frac{b_3}{{\omega_r}^{3/2}} + \frac{b_4}{{\omega_r}^2} \quad (4)$$

p = system pressure, Pa
T = temperature, K
ω_r = refrigerant mass fraction
T_{sat} = saturation temperature at system pressure, K
$a_0 through\ b_4$ = empirical correlation constants

At the suction, the liquid refrigerant mass fraction rapidly increases from 0.2 to 0.8 due to the sudden pressure increase. Then after condensation, the refrigerant mass fraction gradually decreases from 0.7 to 0.4 within 35 min because of the pressure decrease.
The liquid refrigerant mass fraction at the discharge slightly decreases within the 2 min after shutdown, then gradually increases from 0.17 to 0.37 in 40 min. The refrigerant solubility variation at the discharge is determined by the pressure variation.

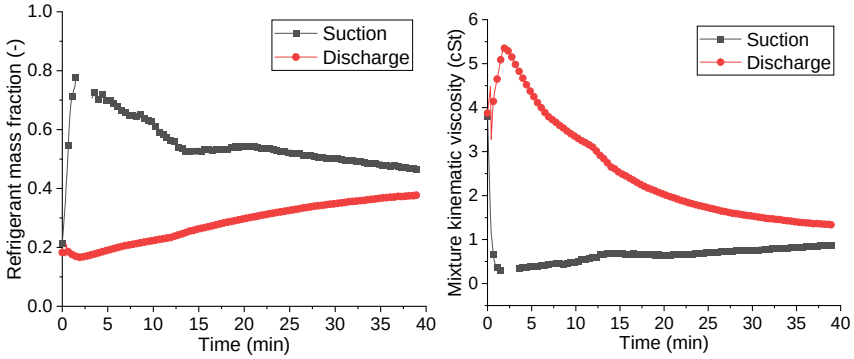

Figure 5. Mixture property variations at compressor suction and discharge

The liquid mixture kinematic viscosity is calculated based on the refrigerant mass fraction and the temperature according to the empirical model developed by Seeton and Hrnjak (2009). The equation and constants used are illustrated in Wang *et al.* (2022). The mixture kinematic viscosity at suction largely drops from 3.8 cSt to 0.3 cSt within 1.5 min after shutdown, which is mainly influenced by the refrigerant mass fraction increase. The temperature increase also contributes to the viscosity decrease. During condensation, the liquid kinematic viscosity is unable to be predicted due to the lack of refrigerant mass fraction data. However, since the liquid refrigerant kinematic viscosity is much lower than the lubricant, it can be inferred that the mixture kinematic viscosity will largely decrease. After the condensation process, because of the temperature and refrigerant solubility increase, the mixture kinematic viscosity gradually increases to 1 cSt within 35 min.
At the discharge, the mixture kinematic viscosity increases from 3.9 cSt to 5.4 cSt within 2 min after shutdown. The variation is caused by the refrigerant mass fraction and temperate decrease. After that, the kinematic viscosity increases because of the solubility increase.
From the mixture property variations, it can be predicted that the oil at the suction rapidly absorbs the vapor refrigerant after shutdown. Meanwhile, the refrigerant condenses at the inner wall of the tube and vaporizes within 10 min after shutdown. The viscosity and surface tension both acutely decrease because of the refrigerant mass fraction increase in the liquid phase. To maintain enough lubrication inside the compressor during restart, the viscosity should remain high during shutdown. Considering the refrigerant migration and condensation at the suction after shutdown, the valve between the evaporator and compressor should be closed immediately after shutdown to stop refrigerant migration into the compressor. In that case, only limited refrigerant would dissolve into the oil inside the compressor, viscosity and surface tension of the mixture could remain high during restart.
At the discharge, the refrigerant stays superheated after shutdown. The refrigerant solubility slightly decreases then increases gradually. Therefore, the mixture kinematic viscosity and surface tension remain high within 5 min after shutdown, and the oil droplet can stay in its original shape for a long time. The flow visualization of the flow at the suction and the discharge proves the predictions.

3.1.3 Flow Visualization: The flow behaviors after shutdown are observed at the suction as shown in Figure 6. Before the shutdown, the flow consists of vapor refrigerant flow and oil annular mist flow. Figure 6 (a) shows that the oil film stops waving after shutdown and breaks from the top of the tube. The liquid droplets with high fluidity appear at the tube wall after 10 s as shown in Figure 6 (b). The liquid can be oil mixture with large portions of vapor refrigerant and condensed liquid refrigerant. The liquid flows down and accumulates at the bottom of the tube. As shown in Figure 6 (c), the liquid level reaches the maximum of 2.2 mm from the bottom of the tube outer wall within 20 s after shutdown. The liquid level starts to decrease gradually 30 s after shutdown as shown in Figure 6 (d), which indicates the liquid refrigerant saturation and the vapor refrigerant desorption.

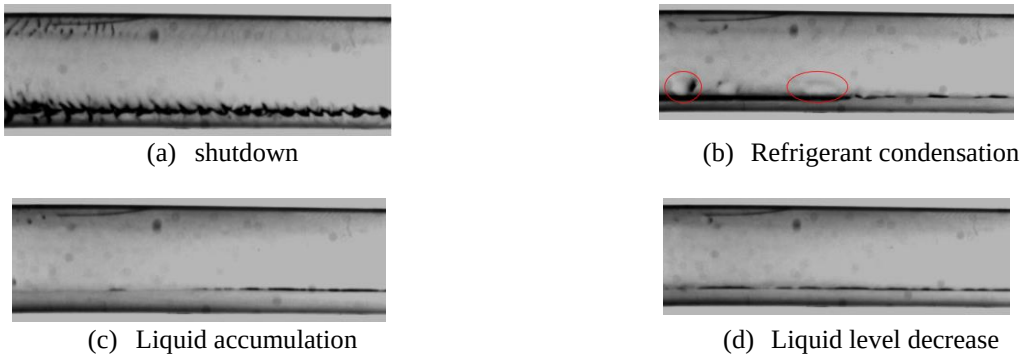

(a) shutdown (b) Refrigerant condensation

(c) Liquid accumulation (d) Liquid level decrease

Figure 6. Flow visualization at compressor suction after shutdown

The flow behavior at the suction is consistent with mixture property variations. The superheat suddenly drops to 0 °C within 1 min after shutdown. As observed, the liquid with low viscosity and surface tension occurs and flows down to the inner wall of the tube. The superheat increases to above 0 °C after 2 min with liquid level decrease.

At the discharge, before the shutdown, the oil flow is composed of small oil droplets in the vapor core and oil streams and droplets attached to the inner wall of the tube. The oil droplets in the vapor core were more than 2 orders of magnitude faster than the oil streams attached to the wall. Because of the low OCR and the low gas superficial velocity, the oil was not able to form uniform oil film in the tube wall.

As shown in Figure 7 (a), the oil stream stops and disperses into oil droplets within 1 s after shutdown, while the oil droplet still travels because of the much higher initial velocity. After 0.5 s, as shown in Figure 7 (b), the oil mist stops traveling with vapor refrigerant and coalesces into oil droplets as shown in Figure 7 (c). The droplets flow down due to gravity slowly then as shown in Figure 7 (d).

The droplets show the “tear-like” phenomenon during shutdown in Figure 7. The same phenomenon was observed by Worsoe-Schmidt (1960) and explained with the surface tension effect. In addition, Manwell and Steven (1990) argued oil viscosity change contributed more to “tearing” at the temperature range (0-40 °C). Wongwises *et al.* (2002) believed the tear-flowing process might be related to the mixture viscosity and wettability. Although the wettability (contact angle) of PFA surface with R134a-PAG 46 mixture was not measured or evaluated before, as a reference, Fukuta *et al.* (2022) evaluated the wettability of metal surfaces with refrigerant-oil mixture by measuring the contact angle of the mixture. It is found that the contact angle of the mixture decreases with increasing refrigerant concentration. However, the spread speed of droplets was influenced by tube material because of different solid surface energy.

According to the refrigerant mass fraction and mixture viscosity variation, the wettability is supposed to increase within 2 min after shutdown and then decrease. The viscosity and surface tension increase and then decrease at the same time. The flow visualization shows the oil droplets keep in their original shape for 5 min and maintain high viscosity and surface tension. Later, as discharge pressure and temperature decrease, the refrigerant mass fraction increases gradually. The oil droplets flow down and accumulate at the bottom of the tube.

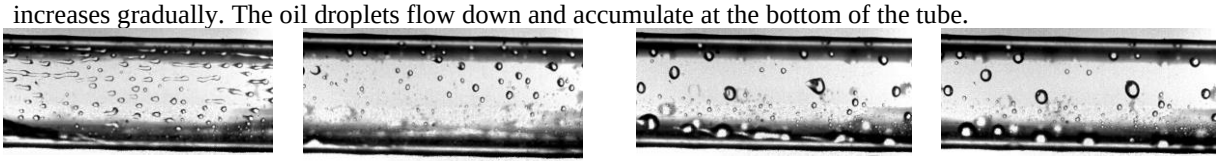

(a) Shutdown (b) Small oil droplets (c) Large oil droplets (d) Oil droplets flow down

Figure 7. Flow visualization after shutdown at compressor discharge

3.2 Compressor Suction Flow Characteristics

To further study the influence of temperature and pressure on property variations and flow behaviors, 3 cases with different initial conditions after shutdown are tested. The working conditions during system operation (before shutdown) for the 3 cases are shown in Table 2. The suction and discharge pressure and temperature increase from Condition A to Condition C, which results in different initial conditions after shutdown. Air-side indoor and outdoor temperatures also increase from Condition A to Condition C as shown in Table 2, which represents different climate conditions. The system is shut down after a steady state is reached and maintained for at least 1 hour in each condition. The working condition and mixture property variations are recorded and estimated after shutdown. Suction flow behavior is observed and analyzed with flow visualization and analysis software.

Table 2. Working conditions before shutdown

	Condition A	Condition B	Condition C
Suction pressure (kPa)	398	403	417
Suction temperature (°C)	22.8	23.1	23.6
Air-side temperature (indoor) (°C)	25.6	26.0	26.8
Discharge pressure (kPa)	841	989	1313
Discharge temperature (°C)	56.6	61.8	72.3
Air-side temperature (outdoor) (°C)	32.6	38.7	49.6

3.2.1 Working Conditions: The temperature and pressure variation in the 3 conditions are shown in Figure 8 and concluded in Table 3. The suction pressure increases 71%, 84% and 104% within 3 min after shutdown and reaches maximum value in Condition A, B and C. The difference in pressure increasing rate is caused by different compression factors at steady state. Since the initial discharge pressure in Condition C is much higher than that in Condition A and B, the suction pressure increases most quickly after shutdown during the pressure equilibrium period.

Table 3. Working condition variations after shutdown at compressor suction

	Condition A	Condition B	Condition C
Maximum suction pressure/steady state pressure (kPa)	1.7	1.8	2.0
Maximum suction temperature increase (°C)	4.3	5.6	9.8

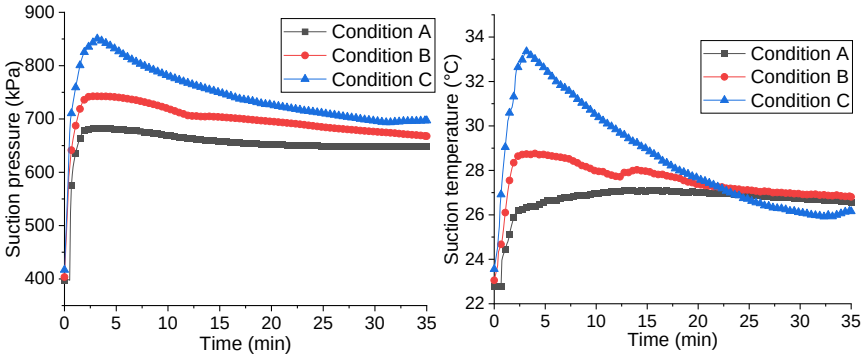

Figure 8. Pressure and temperature variations at compressor suction

The suction temperature increases by 4.3, 5.6 and 9.8 °C in Condition A, B and C after shutdown. The suction temperature in Condition C increases most acutely. Although the initial suction temperatures are similar in the 3 conditions, the discharge temperature in Condition C is much higher. As hot refrigerant migrates to the low-pressure side, the suction temperature increases at different rates among the 3 conditions.

As explained before, the pressure and thermal equilibrium reach asynchronously at suction. Therefore, the difference between suction temperature and saturation temperature decreases dramatically after shutdown as shown in Figure 9. The temperature difference drops to 0.1 °C in Condition A within 1 min after shutdown but stays above 0 °C in the whole process. In Condition B, the temperature difference drops to slightly below 0 °C within 3 min after shutdown,

then increases gradually. Nonetheless, in Condition C, the temperature quickly drops to below 0 °C in 0.5 min after shutdown and continues for 6 minutes. After that the temperature difference briefly increases to slightly above 0 °C for 7 minutes, then decreases to below 0 °C again.

Considering the temperature difference between the measured vapor core and the tube wall as well as the uncertainty of the devices, it can be inferred that the condensation occurs in all 3 conditions. However, Condition C is supposed to derive longer and more severe condensation.

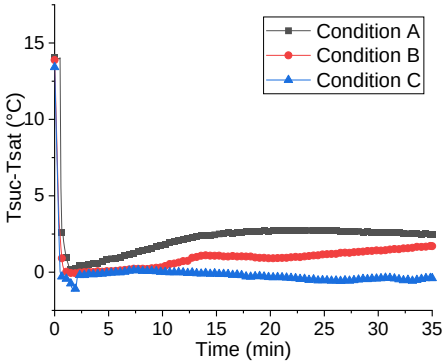

Figure 9. Superheat and subcooling at compressor suction

3.2.2 Mixture Properties: The refrigerant solubility and mixture kinematic viscosity variations are shown in Figure 10 and Table 4. Due to the limitation of the refrigerant mass fraction model, Condition B and C have gaps in refrigerant mass fraction and mixture kinematic viscosity curves. The refrigerant mass fraction increases rapidly after shutdown. In Condition A, the refrigerant mass fraction reaches the maximum value as 0.67 within 1.5 min then gradually decreases. Condition B refrigerant mass fraction reaches 0.78 before condensation happens. After condensation, the refrigerant mass fraction gradually decreases. In Condition C, the refrigerant mass fraction rapidly increases to 0.7 within 20 s before condensation, then fluctuates at 0.7 and finally increases to 0.83 after condensation. After 12 min, the condensation happens again. Although Condition B and C curves are incomplete because of the limitation of the model, it is still evident that the refrigerant mass fraction in the liquid phase increases from Condition A to C.

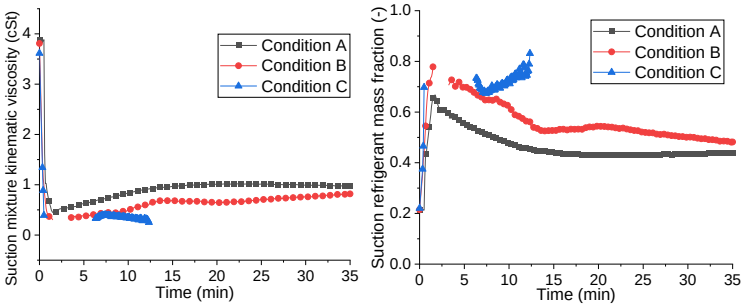

Figure 10. Mixture property variations at compressor suction

The mixture kinematic viscosity is determined by the refrigerant mass fraction and the temperature. Because of the sudden increase in refrigerant mass fraction and temperature, the kinematic viscosity decreases rapidly and then gradually increases. The variation of mixture kinematic viscosity is shown in Table 4. Among the 3 conditions, the minimum kinematic viscosity is smallest in Condition C because of the highest refrigerant mass fraction and suction temperature. During condensation, the liquid refrigerant mixes with oil along with the absorbed vapor refrigerant. Therefore, the liquid viscosity should be even lower than that in superheated conditions.

The solubility variations in the 3 conditions show that with higher indoor and outdoor temperatures during operation, more refrigerant will condense and be absorbed by the same amount of oil inside the compressor after shutdown. As a result, the mixture viscosity will decrease even more in Condition C. During the longer shutdown time, the absorbed refrigerant might migrate to the evaporator and condenser, which will carry oil out of the compressor. To avoid oil migration and lack of lubrication, the valve at the compressor inlet and outlet should be closed quickly after shutdown.

Table 4. Mixture kinematic viscosity variation after compressor shutdown

	Condition A	Condition B	Condition C
Minimum mixture kinematic viscosity (cSt)	0.43	0.3	0.25
Decrease scale	89%	92%	93%

3.2.3 Flow Visualization: The flow behavior after shutdown is observed at the suction for the 3 conditions. The flow behaviors are similar among the 3 conditions, as the oil film stops moving, it breaks from the top of the inner wall. The condensation occurs in all 3 conditions, but lasts longer and causes more liquid accumulation in Condition C. As shown in Figure 11, the maximum liquid levels measured from the tube outside in Condition A, B and C are 2.18 mm, 2.20 mm, and 2.24 mm.

The liquid levels stay constant for around 0.5 min and then decrease quickly, which reflects the saturation of the liquid refrigerant and vapor refrigerant desorption.

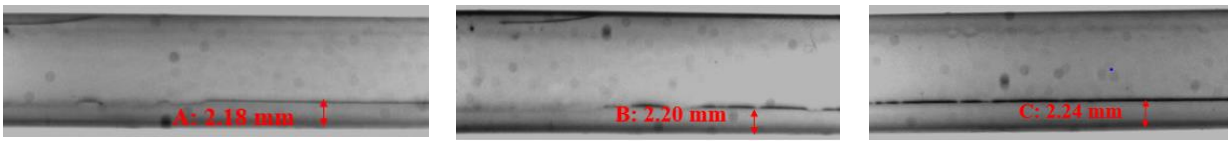

Figure 11. Flow visualization at compressor suction after shutdown

4. CONCLUSIONS

Different flow behaviors and mixture property change after shutdown at the compressor suction and discharge are studied. Three climate conditions are tested to compare after shutdown at suction. At suction, oil film breaks from the top of the tube wall then flows down quickly. Refrigerant condenses at the tube wall momentarily because of the asynchronous nature of the pressure and thermal equilibrium. As flow visualization shows, the liquid level increases because of the condensation and refrigerant absorption. After a short time, the liquid level decreases as the refrigerant vaporizes and escapes from oil. The sudden increase of refrigerant solubility and sudden decrease of mixture kinematic viscosity explain the flow visualization results. At discharge, the refrigerant mass fraction decreases slightly then increases, and the mixture kinematic viscosity increases then decreases gradually. As a result, the flow visualization shows that oil remains at the tube wall as oil droplets for a longer term, then flows flow down due to gravity.Among the 3 tested conditions, at suction, the pressure and temperature change most rapidly with higher initial pressure and temperature, the condensation occurs faster and more severely as well. The maximum liquid level is higher and maintained longer. The refrigerant condensation and mass fraction change can largely affect mixture viscosity, surface tension and wettability. To protect compressor and improve oil return during restart up, the compressor should be separated from the rest of the system to reduce refrigerant absorption and oil migration.

NOMENCLATURE

A(ω_r)	coefficient of solubility	
a_0 through a_1	coefficients	
B(ω_r)	coefficient of solubility	
b_0 through b_4	coefficients of solubility	
COP	coefficient of performance	
OCR	oil circulation ratio	
p	pressure	(kPa)
T	temperature	(K)
ρ	density	(g/cc)
ω	mass fraction of component in refrigerant-oil mixture	
Subscript		
*	non-dimensional saturation temperature	
r	refrigerant	

sat	saturation
suc	suction

REFERENCES

Cremaschi, L., Hwang, Y., & Radermacher, R. (2005). Experimental investigation of oil retention in air conditioning systems. *International Journal of Refrigeration*, *28*(7), 1018-1028.

Fukuta, M., Sumiyama, J., Motozawa, M., & Chaiworapuek, W. (2020). Wettability of metal surface with oil/refrigerant mixture. *International Journal of Refrigeration*, *119*, 131-138.

Grebner, J. J. (1992). The effects of oil on the thermodynamic properties of dichlorodifluoromethane (R-12) and tetrafluoroethane (R-134a). *Air Conditioning and Refrigeration Center TR-13*.

Haider, S. A. (2023). Commissioning of experimental facility for oil circulation rate measurements in a vapor compression system (Doctoral dissertation, University of Illinois at Urbana-Champaign).

Haider, S. A., Wang, X., & Elbel, S. (2023a). Measurements of Oil Circulation Rate using Flow-through and Evacuated Type Sampling Cylinders for an Automotive Air Conditioning System (No. 2023-01-0138). SAE Technical Paper.

Haider, S. A., Wang, X., & Elbel, S. (2023b). Study of Flashing Flows Entering Evacuated Sampling Cylinders for Oil Circulation Rate Measurement in an Automotive Air Conditioning System (No. 2023-01-0140). SAE Technical Paper.

Manwell, S. P. (1990). Gas-Liquid Flow Patterns in Refrigerant Oil Mixtures. *ASHRAE transactions*, *96*, 456-464.

McMullan, J. T., Hewitt, N. J., Masson, A. J., & Murphy, N. E. (1992). The influence of oil viscosity and refrigerant quality on evaporator performance. *International journal of energy research*, *16*(7), 567-581.

Peuker, S. (2010). *Experimental and analytical investigation of refrigerant and lubricant migration*. University of Illinois at Urbana-Champaign.

Radermacher, R., Cremaschi, L., & Schwentker, R. A. (2006). Modeling of oil retention in the suction line and evaporator of air-conditioning systems. *HVAC&R Research*, *12*(1), 35-56.

Seeton, C. J., & Hrnjak, P. S. (2009). CO2-lubricant two-phase flow patterns in small horizontal wetted wall channels: The effects of refrigerant/lubricant thermophysical properties. *Urbana*.

Sethi, A., & Hrnjak, P. (2015). Modeling of oil retention and pressure drop in vertical suction risers. *Science and Technology for the Built Environment*, *21*(7), 1033-1046.

Stevanovic, V. D., & Hrnjak, P. (2017). Numerical simulation of three dimensional two-phase flow and prediction of oil retention in an evaporator of the automotive air conditioning system. *Applied Thermal Engineering*, *117*, 468-480.

Wang, X., Haider, S. A., Hrnjak, P., & Elbel, S. (2022). Transient Oil-refrigerant Mixture Migration and Change of Properties at Compressor Shutdown. *Proceedings of the International Refrigeration and Air Conditioning Conference*, Paper 2265, West Lafayette, IN, USA.

Wang, X., Haider, S. A., & Elbel, S. (2023). Transient Oil Migration and Flow Behavior during Automotive Compressor Startup (No. 2023-01-0142). SAE Technical Paper.

Wongwises, S., Wongchang, T., Kaewon, J., & Wang, C. C. (2002). A visual study of two-phase flow patterns of HFC-134a and lubricant oil mixtures. *Heat Transfer Engineering*, *23*(4), 13-22.

Worsoe-Schmidt, P. (1960). Some Characteristics of Flow Pattern and Heat Transfer of Fren 12 Evaporation in Horizontal Tubes. *The J of Refrigeration*, *3*(2), 40-44.

Xu, J., & Hrnjak, P. (2017). Quantification of flow and retention of oil in compressor discharge pipe. *International journal of refrigeration*, *80*, 252-263.

ACKNOWLEDGEMENT

The authors would like to thank the member companies of the Air Conditioning and Refrigeration Center at the University of Illinois at Urbana-Champaign for their funding to support this project, Bergstrom for compressor, Sanhua for EEV, and Creative Thermal Solutions for the technical support.